

Water Resources Research®

RESEARCH ARTICLE

10.1029/2025WR040324

Quantifying Changes in Water Loading in the U.S. Southwest via Comparison of GNSS, GRACE, and SWE Data Sets



Key Points:

- Comparison of several geodetic data sets showcases seasonal hydrological partitioning in the Colorado River Basin
- Mountainous locations are sensitive to snowpack changes, while locations down basin are sensitive to river and lake hydrology
- The Wasatch Range, Southern Rocky Mountains, and lower Colorado River Basin act as hydrologically distinct sub-regions in geodetic data sets

Supporting Information:

Supporting Information may be found in the online version of this article.

Correspondence to:

K. C. Gourley,
kengourley@arizona.edu

Citation:

Gourley, K. C., Bennett, R. A., & Harig, C. (2026). Quantifying changes in water loading in the U.S. Southwest via comparison of GNSS, GRACE, and SWE data sets. *Water Resources Research*, 62, e2025WR040324. <https://doi.org/10.1029/2025WR040324>

Received 24 FEB 2025

Accepted 26 JAN 2026

Author Contributions:

Conceptualization: Richard A. Bennett, Christopher Harig

Data curation: Kenneth C. Gourley

Formal analysis: Kenneth C. Gourley

Funding acquisition: Christopher Harig

Investigation: Kenneth C. Gourley

Methodology: Kenneth C. Gourley,

Richard A. Bennett, Christopher Harig

Project administration: Richard

A. Bennett, Christopher Harig

Software: Kenneth C. Gourley, Richard A. Bennett

Supervision: Richard A. Bennett, Christopher Harig

Validation: Kenneth C. Gourley

Visualization: Kenneth C. Gourley

© 2026 The Author(s).

This is an open access article under the terms of the [Creative Commons](https://creativecommons.org/licenses/by/4.0/)

[Attribution-NonCommercial](https://creativecommons.org/licenses/by/4.0/) License,

which permits use, distribution and reproduction in any medium, provided the original work is properly cited and is not used for commercial purposes.

Kenneth C. Gourley¹ , Richard A. Bennett^{1,2} , and Christopher Harig¹

¹Department of Geosciences, The University of Arizona, Tucson, AZ, USA, ²Now at NOAA National Geodetic Survey, Silver Spring, MD, USA

Abstract We use geodetic data to show that hydrologically distinct sub-regions in the Southwest United States act independently of one another. The limited number of Global Navigation Satellite System (GNSS) stations and resolution of Gravity Recovery and Climate Experiment (GRACE) make hydrological partitioning difficult to unravel, especially in the Colorado River Basin which comprises a diversity of climates due to its highly variable topography. Here, we compare GNSS station vertical displacement data, GRACE surface mass change data, and snow water equivalent (SWE) data using elastic surface displacement modeling and signal localization techniques. We focus on a region composed of Arizona, New Mexico, Colorado, and Utah, allowing for the examination of variations in the Colorado River Basin, the primary source of water for the region's municipalities, agriculture, and ecosystems. We demonstrate that the accumulation and melt of snow have a first-order control on the timing of vertical displacement in this region. There exists a region-dependent seasonal partitioning between when GNSS and GRACE sense changes in the distribution of terrestrial water storage. In the Wasatch Range of central Utah, GNSS stations sense loading due to changes in the snowpack one to 2 months in advance of GRACE; in the Southern Rocky Mountains of Colorado, GNSS stations sense loading due to changes in the snowpack one to 3 months in advance of GRACE; and in the lower Colorado River Basin of Arizona, GRACE senses loading due to changes in river runoff three or more months in advance of GNSS stations.

Plain Language Summary As water and snow accumulate and redistribute on the Earth's surface, the crust moves elastically in response, similar to placing weights on or removing weights from a rubber band. This elastic motion due to changes in terrestrial water storage (including glaciers, snow cover, lakes, rivers, and groundwater) is small (sub-millimeter to several millimeters per year) but can be measured with modern geophysical techniques. This includes the Global Navigation Satellite System (GNSS): a network of sensors installed to measure 3D deformation of the Earth's surface. Another similar technique is the Gravity Recovery and Climate Experiment (GRACE/GRACE-FO), two satellite missions that measure changes in the Earth's gravity field to estimate surface mass, which largely reflects terrestrial water storage. In this study, we combine measurements from both techniques with existing estimates of the North American snowpack from 2002 to 2024 to quantify watershed-basin-scale hydrological features in the southwestern United States. In particular, we observe a difference in timing of when GNSS versus GRACE is able to sense the distribution of water in various parts of our region. We attribute this to the seasonal storage of water as snow and ice in the mountainous parts of the region.

1. Introduction

Monitoring and quantifying changes in terrestrial water storage (TWS) throughout the Western United States is essential to water-related policies regarding current and future droughts. Existing measures of drought intensity do not take into account water availability from snow, which is an important driver of hydrological variations in this region (Adusumilli et al., 2019). Geodetic measurements of TWS are produced through the Gravity Recovery and Climate Experiment and the later follow-on (GRACE and GRACE-FO) missions, which determine global gravity variations at monthly intervals (Tapley et al., 2004). Over land, these time-variable gravity fields reflect hydrologic, cryospheric, and atmospheric mass redistribution at monthly and inter-annual time scales and at spatial scales greater than 300 km (Landerer & Swenson, 2012; Swenson & Wahr, 2006). The calculation of the Earth's response to hydrologic loads using Global Navigation Satellite System (GNSS) stations can help

Writing – original draft: Kenneth C. Gourley
Writing – review & editing: Kenneth C. Gourley

complement the limited spatiotemporal resolution of GRACE TWS measurements (Blewitt et al., 2001; Tregoning & Watson, 2009).

Variations in water, snow, and ice on the Earth's surface result in deformation of the topographic and geoidal shapes of the Earth (Han & Razeghi, 2017). Such variations in TWS have strong periodic components that produce a mostly elastic response (Farrell, 1972) which appears in both the horizontal and vertical components of GNSS station time series (e.g., van Dam et al., 2007). For regions in which secular changes in TWS occur, the vertical component of GNSS station time series can further be utilized to estimate the magnitude of these perturbations (e.g., Argus et al., 2017; Knowles et al., 2020). When combined with GRACE TWS data, these GNSS vertical displacement data can be used to estimate both the periodic and secular variations in TWS at a finer spatiotemporal scale in a specific region than that available from GRACE alone (Davis et al., 2004; Knappe et al., 2019). Accompanying these benefits, interpretation of GNSS data for hydrogeodetic applications is complicated by a range of potential sources of periodic motions, such as thermoelastic and poroelastic deformation of the area surrounding the site and environmental effects (e.g., Bogusz et al., 2024; Chanard et al., 2020; Dong et al., 2002), that are presently not well understood and for which there is currently no consensus. In addition to a variety of physical processes, processing methods and analysis models may also contribute to periodic signals observed in GNSS coordinate time series data (e.g., Ray et al., 2007). Bogusz et al. (2024) noted a worldwide annual common mode between IGS Repro3 (Rebischung et al., 2024) and UNR coordinate time series differences, with a median amplitude of the order of 2 mm, peaking in the late summer, which may be explained by different frame realization strategies. These caveats aside, GNSS's contributions to hydrogeodesy are far reaching (e.g., White et al., 2022, and references therein).

While the temporal resolution for an analysis that combines GNSS vertical displacement data and GRACE TWS data can be refined to a daily interval, the spatial resolution is highly dependent on the GNSS station density within a particular region (Adusumilli et al., 2019; Knappe et al., 2019). Studies within regions that have high station densities, such as California, are able to determine TWS changes down to a scale of 10–20 km (Argus et al., 2014, 2017; Carlson et al., 2022). For regions with much sparser station coverage, TWS changes are still resolvable down to a resolution of 50–100 km (Han & Razeghi, 2017). Neither geodetic measurement is optimal for monitoring individual watersheds, but the length scales of their sensitivities prove to be complementary.

Joint analysis has been performed for several regions besides California, including Oregon and Washington (Fu et al., 2015), the Northern Rockies (Knappe et al., 2019), the Amazon Basin (Davis et al., 2004; Knowles et al., 2020), and Australia (Han & Razeghi, 2017). Such studies are able to find good agreement between GNSS vertical displacement data and GRACE TWS data away from mountain ranges. In mountainous regions, including most of the Western United States, several studies incorporate independent measurements of the local snowpack in order to improve their analyses (Argus et al., 2014; Enzlinger et al., 2019; Fu et al., 2015; Knappe et al., 2019; Ouellette et al., 2013). When using geodetic data to estimate TWS in such regions, it is necessary to use an accurate snowpack model, as snow water equivalent (SWE) is the dominant signal in those time series (Enzlinger et al., 2018). This is especially important when there are other competing hydrological signals, such as those from aquifers, that may be out of phase and combine destructively with the SWE signal (Argus et al., 2014, 2017). In the mountainous western U.S., SWE is estimated from a combination of remote sensing, in situ measurements, and models. All three methods suffer from the high spatial heterogeneity of snow accumulation and density (Enzlinger et al., 2018). For example, in situ measurements, such as snow telemetry (SNOTEL), have the highest spatial resolution, but they cannot be applied over an entire region due to the uneven nature of snow accumulation at even the kilometer scale (Serreze et al., 1999).

Recent literature reviews of hydrogeodesy highlight several outstanding questions in the field, including how to improve the spatial resolution of TWS estimates to learn more about hydrologic partitioning (Jaramillo et al., 2024; White et al., 2022). The largest watershed in the Southwest United States is the Colorado River Basin (pink outline in Figure 1), where water is partitioned between snow, ice, groundwater, rivers, and lakes. The snow and ice accumulate in mountain regions during the fall and winter and then melt during spring and summer. These seasonal changes in the snowpack dominate the GRACE TWS data set in this region, and, combined with the rough spatial resolution of this data set, it is difficult to examine hydrological partitioning with GRACE alone. In order to extract sub-watershed-scale information about the Colorado River Basin, it is necessary to incorporate other geodetic data sets, such as GNSS.

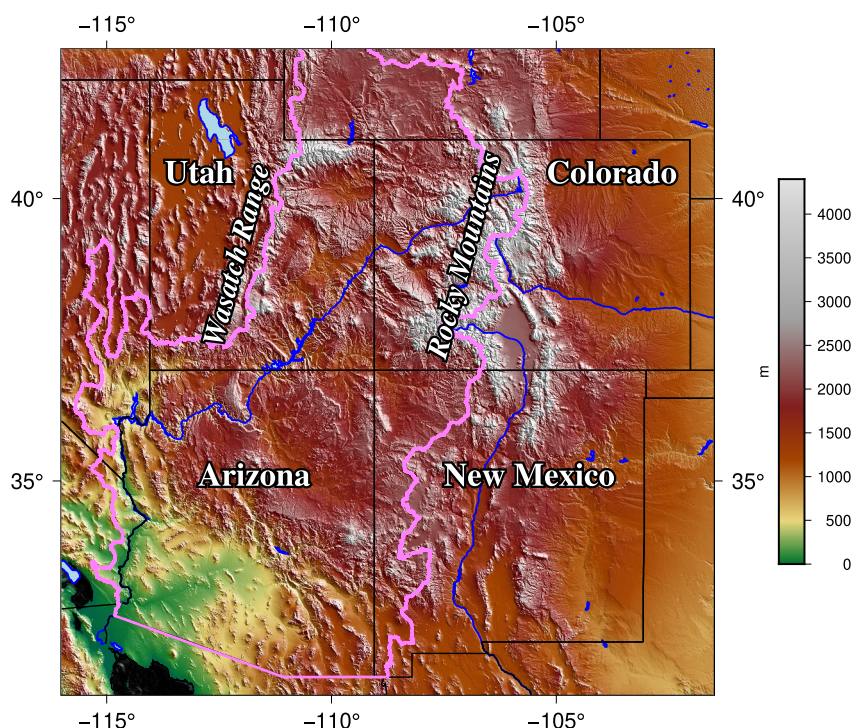


Figure 1. Plot of the surface topography of the Southwest United States. The black lines are state and federal borders; the blue lines are major rivers; and the pink line is the boundary of the Colorado River Basin. The study region—composed of the states of Arizona, New Mexico, Colorado, and Utah—contains varying elevations and multiple mountainous areas. The major rivers in the study region are the Colorado (center), Arkansas (center right), and Rio Grande (bottom right). The mountain ranges which accommodate the majority of the fall and winter snowpack are the Rocky Mountains, which extend through central and western Colorado and northern New Mexico; and the Wasatch and Uinta Ranges, which extend from central to northern Utah. These same ranges also supply snowmelt to the upper Colorado River Basin, which then flows down to the Gulf of California (Zeng et al., 2018).

In this study, we compute statistical comparisons of GRACE TWS, GNSS vertical displacement, and SWE data sets in the Southwest United States (Figure 1) to demonstrate how to enhance the spatial resolution of TWS estimates in mountainous regions. Although previous work has created a refined TWS model using GRACE and GNSS data sets for the conterminous United States (Adusumilli et al., 2019), little attention has been paid to the seasonality of hydrologic partitioning between mountains and rivers. Additionally, the spacing of continuously operating GNSS stations is irregular in this region, making regional variations difficult to observe. We overcome this challenge by using a data localization technique based on Slepian basis functions (Harig & Simons, 2012; Simons & Dahlen, 2006). We demonstrate regional- and watershed-scale changes in TWS and quantify the contribution of the snowpack SWE signal to the overall GRACE TWS model for the study region.

2. Data

2.1. GNSS Displacements

We use GNSS displacements from 266 heterogeneously spaced, continuously operating stations across Arizona, New Mexico, Colorado, and Utah (Figure 2). Most of these stations were installed between 2005 and 2010. The final orbit daily GNSS solutions for vertical displacement were processed by the University of Nevada Reno's Nevada Geodetic Laboratory (UNR; <http://geodesy.unr.edu/>). These solutions were generated using GipsyX utilizing the Jet Propulsion Laboratory's orbital products, the FES2004 ocean tide model, and solid Earth tides from IERS 2010 conventions. We use daily positions products given in the International Terrestrial Reference Frame 2014 (Altamimi et al., 2016). Further information on the processing method utilized by UNR can be found in Blewitt et al. (2018). The precision of the vertical signal varies daily for each station, with formal error usually 1–2 mm, and these daily uncertainties are propagated into the time series.

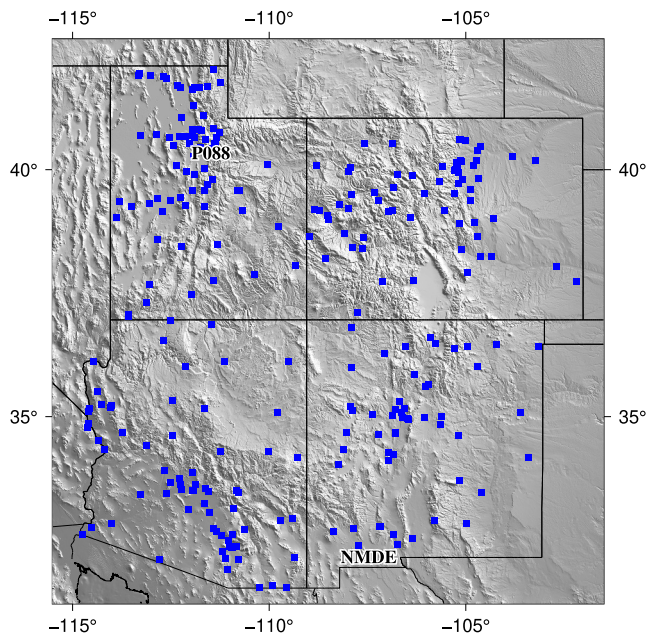


Figure 2. Map of the study region topography with the GNSS station locations used in this study plotted as blue squares. The stations NMDE (lower center) and P088 (upper left), whose time series are plotted in Figure 3, are labeled. Station density is high in most mountainous parts of this region, as well as in the Basin and Range. However, station coverage is not uniform and is quite poor on the Colorado Plateau and in the eastern parts of Colorado, Utah, and New Mexico.

After downloading the GNSS station data, we use Hector (<http://segal.ubi.pt/hector/>) to remove outliers and jumps from each station's vertical displacement time series (Bos et al., 2013). Outliers are single data points that fall outside of the statistical trend of each station's time series and, in Hector, are defined as more than three times the interquartile range above or below the median value of each time series. Jumps are sudden shifts in the statistical trend that can come from a variety of sources, primarily earthquakes and changes in station antennas. Outliers and jumps frequently plague GNSS station time series, and their removal greatly improves the intercomparisons with the GRACE and UASWE displacement time series used in this study (e.g., Enzinger et al., 2019; White et al., 2022).

2.2. GRACE Time-Variable Gravimetry

We use monthly GRACE RL-06 and GRACE Follow-On RL-06.2 data (collectively referred to as GRACE data in this paper) from the Center for Space Research at the University of Texas at Austin. These data are distributed as Stokes coefficients to degree and order 60. The GRACE data span from April 2002 to February 2024, with 37 missing months due to satellite operations and the gap between the missions. Degree 2 and 3 order 0 coefficients are replaced with those from GRACE Technical-Note 14, which are derived from satellite laser ranging (Loomis et al., 2020). Degree 1 coefficients are added from GRACE Technical-Note 13, representing estimated geocenter variations (Sun et al., 2016; Swenson et al., 2008). We transform the geopotential into surface mass density using the method of Wahr et al. (1998) to account for the surface deformation resulting from surface mass changes. We do not apply a correction for glacial isostatic adjustment here, as we are only analyzing seasonal variations and de-trend all data (see Section 3.1).

We localize the GRACE data to the study region using Slepian functions (Harig & Simons, 2012; Simons & Dahlen, 2006). The study region here is defined by the area enclosed by the combined governmental borders of the four Colorado Plateau states: Arizona, New Mexico, Colorado, and Utah (Figure 1). We also include a 0.5° buffer around the region to mitigate any effects from GNSS stations very near the region boundary. This Slepian method allows for the spatio-spectral concentration of data within in an arbitrary region on a sphere and has been successfully applied to GRACE data to study mass changes in ice sheets and mountain glaciers (e.g., Beveridge et al., 2018; Harig & Simons, 2015, 2016; von Hippel & Harig, 2019). Each Slepian function is a solution to an eigenvalue equation that optimizes the localization within a region. Essentially, the Slepian method projects the global signal into a new basis which is optimized for the region of interest. The associated eigenvalue is a measure of the global signal's concentration within this region. We create this new Slepian basis using only the well-concentrated functions with the corresponding highest eigenvalues within this region. This results in a sparse representation of data, as significantly fewer functions are required to represent the regional signal. This allows for the creation of models that experience very little influence from phenomena outside of the region of interest. The localized surface density fields are then expanded on a 0.25° grid for use with LoadDef (Martens et al., 2019).

2.3. Snow Water Equivalent Product

The University of Arizona snow water equivalent product (UASWE) (Zeng et al., 2018) data set is composed of daily measurements of SWE across the conterminous US. These measurements are given on a regularly spaced grid with a resolution of 4 km. The data span from October 1981 to September 2023, although this study focuses on the subset of measurements that overlaps in time with GRACE data. We use this SWE data set because of its high spatial and temporal resolutions and its full coverage of the conterminous U.S. during our full time period of interest. The UASWE data set is constructed by assimilating in situ measurements of SWE and snow depth with precipitation and temperature data across the conterminous U.S. Specifically, Zeng et al. (2018) combine in situ point measurements of SWE with estimates of snow cover extent and snow depth derived from remote sensing across thousands of sites. The point measurements of SWE are interpolated based on precipitation and

temperature data measured at in situ SWE station locations and then combined with gridded daily precipitation and temperature data to expand the daily product across the entire conterminous U.S (Broxton et al., 2016).

Similar to our processing of GRACE data, we project the UASWE spatial fields into the same $L = 60$ Slepian basis localized to the four state study region. This spatially bandlimits the UASWE data set for consistent comparison between the two data sets. The regionalized data set is then re-gridded at a regular interval of 0.25° for use in LoadDef.

3. Methods

3.1. Conversion to Displacement Measurements and Time Series Modifications

We use the software package LoadDef (<https://github.com/hrmartens/LoadDef>) to compute vertical surface displacements resulting from the regionalized GRACE and UASWE surface mass distribution data sets (Martens et al., 2019). LoadDef produces analytical models of surface mass loading for a spherically symmetric, non-rotating, elastic, and isotropic planet (Martens et al., 2019). Load Love numbers (Love, 1909) are computed based on a model of densities and seismic-wave velocities for Earth as a function of radius; PREM (Dziewonski & Anderson, 1981) is chosen as the model for both parameters in this study. Load Green's functions (Farrell, 1972) are then computed based on the load Love numbers. Lastly, to derive the surface displacement response, the load Green's functions are integrated and multiplied by the gridded load height and density for an input surface mass distribution. This LoadDef Earth model is the same one that we use to compute the surface density of the GRACE time-variable gravity data set. The density of water, $1,000 \text{ kg/m}^3$, is chosen for both GRACE and UASWE, as both data sets are given as a water equivalent. The displacement response for both surface mass distribution data sets is computed at each GNSS station location for easy comparison between all three data sets. Before the UASWE data set is passed as input to LoadDef, the monthly average load is computed using the same monthly endpoints as used by the GRACE data set. This reduces the computational load of running the LoadDef routines for two data sets over 276 months at 266 station locations.

All three time series are temporally smoothed using radial basis functions (RBFs) as smoothing functions followed by interpolation at a daily interval. The RBF routine used is from the scikit-learn software package (<https://scikit-learn.org/>), which optimizes kernels over a range of input time scales (Pedregosa et al., 2011). A range of 0.5–10 years is selected to form the RBF kernels for this study, as this range captures the intra- and inter-annual variations present in all three data sets. These data sets are primarily dominated by a periodicity of 1 year. For consistency between data sets, the same set of RBF kernels is applied to all three vertical displacement time series. This low-pass filtering scheme serves to overcome the challenge presented by small gaps in the daily GNSS station data and monthly gaps in the GRACE data. The kernels also provide a low-pass filter for the data sets, resulting in the suppression of daily and weekly variations in the time series. These variations are likely not the result of elastic surface loading due to changes in hydrology, which is the focus of this study (Adusumilli et al., 2019; Farrell, 1972). After applying the RBF kernels to the three displacement data sets, the time series are then re-sampled at a daily interval.

3.2. Data Intercomparisons

Three new data products are created in this study in order to examine the effects of variations in hydrology on geodetic data sets in the Southwest United States: (a) temporal phase delays between vertical GNSS time series and computed GRACE vertical displacement data; (b) least-squares regressions between vertical GNSS time series and computed UASWE vertical displacement; and (c) least-squares regressions between computed GRACE and UASWE vertical displacement data. Each of these products is evaluated at the 266 GNSS station locations in the study area.

Before creating these products, the common time window for all three displacement data sets is selected at each station location. The time series are then sliced such that only the overlap between the pertinent time series is analyzed. We choose a minimum overlap of 3 years between the GNSS and GRACE time series. This results in short intervals of overlap at some stations when comparing the GNSS and GRACE vertical displacement data sets, as some GNSS stations were deployed relatively recently. These short intervals are a cause of the poor cross-correlation observed when computing the temporal phase delays between these two time series at some station

locations. Each time series is also de-trended by removing the mean and standard deviation before proceeding with computing the temporal phase delays or least-squares regressions.

We compute GRACE-GNSS phase delays to highlight the additional hydrological resolution that vertical GNSS station displacements can provide when compared with GRACE surface water loading data in a specific region. When comparing Figures 3a and 3b, it becomes apparent that the phase delay between the GNSS and GRACE time series is not uniform among station locations. These phase delays are computed by cross-correlating the de-trended GNSS and GRACE vertical displacement data sets. Specifically, the cross-correlation $r(l)$ across all shifts or lags l is calculated as

$$r(l) = \sum_{t=t_0}^{t_1} GNSS(t)GRACE(t-l), \quad (1)$$

where the range $[t_0, t_1]$ is the set of times for which the two data sets overlap; $GNSS(t)$ is the re-sampled and de-trended GNSS data set at a specific station; and $GRACE(t)$ is the re-sampled and de-trended elastic deformation due to changes in GRACE TWS computed at the same GNSS station location. We choose the time delay of the maximum value of $r(l)$ at each station as the corresponding phase delay. Any computed phase delays longer than 6 months are removed. Because the primary periodic signal in both data sets is approximately annual, any computed phase delay longer than half this period is due to poor correlation and not representative of any physical process. The final set of phase delays is then projected into the same local Slepian basis used for the GRACE and UASWE data sets in the study region and plotted.

We compute two regression products by performing a least-squares regression using the UASWE vertical displacement data values as the independent variable for both. These regressions are performed at each station location. One regression uses the GNSS vertical displacement data values as the dependent variable, and the other uses the GRACE vertical displacement data values. To compute these regressions, the re-sampled and de-trended elastic deformation due to changes in UASWE is subtracted from either (a) the re-sampled and de-trended GNSS data set or (b) the re-sampled and de-trended elastic deformation due to changes in GRACE TWS. The corresponding coefficient of determination R^2 for both (a and b) is then computed at each GNSS station location. The resulting R^2 value of fit for the regression at each station location is then the measure of the percentage of variation in the dependent variable that can be explained by variation in the independent variable. This statistical analysis presents a method of determining how strongly GNSS vertical displacement and GRACE TWS are determined by changes in snowpack SWE within the study region. High values of R^2 indicate that snowpack SWE is the dominant driver of surface elastic deformation, while low values indicate that a different physical process must control the displacement at a given location. These two regression products at the stations are then projected into the same Slepian basis as described above and plotted separately.

4. Results

4.1. Phase Delays

The result of the phase delay computation between the GNSS and GRACE vertical displacement data sets is shown in Figure 4. Of the 266 GNSS stations used in this study, 259 produce phase delays through cross-correlation with the GRACE vertical displacement data set. Of these 259 phase delays, only 110 are less than 6 months; these are the phase delays plotted in Figure 4. The phase delays are mostly coherent in the various sub-regions of the study area. In Colorado, phase delays are scattered around -60 days, indicating that GNSS stations in this sub-region sense vertical motion around 2 months in advance of GRACE satellite gravimetry. In Utah, phase delays are scattered around 0 days, with most being slightly negative, suggesting that, in this sub-region, GNSS stations and GRACE satellite gravimetry sense changes in elastic deformation due to surface water loading at around the same time. In Arizona, phase delays are mostly scattered around 90 days, indicating that GNSS stations in this sub-region sense changes in elastic deformation due to surface water loading months after it is perceived by GRACE satellite gravimetry. Phase delays are widely scattered in New Mexico, with many around -120 days and other around 80 days. This suggests that there is little consistency among GNSS station responses in this sub-region.

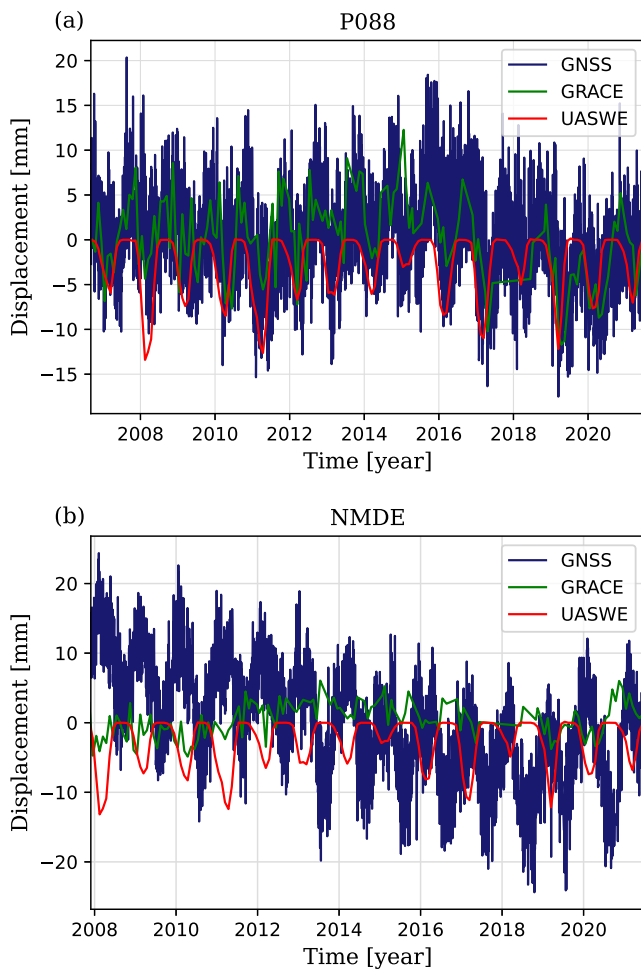


Figure 3. Plot of the vertical displacement time series at GNSS stations (a) P088 and (b) NMDE for the three data sets used in this study. The detrended and de-meaned GNSS daily vertical displacement is plotted in blue, while the computed vertical displacements due to elastic loading (output from LoadDef) from the GRACE TWS and UASWE snowpack SWE data sets are plotted in green and red, respectively. These data sets were not smoothed before plotting. (a) P088 is located in the upper elevations of the Wasatch Range (see Figure 2). The periodic annual amplitude of vertical deformation for the GNSS time series is around ± 15 mm, while the equivalent computed amplitudes for the GRACE and UASWE time series are lower, at ± 8 mm and -10 to 0 mm, respectively. These annual periods are close to being in-phase at this station, with GRACE lagging UASWE by about 20 days and GNSS lagging GRACE by 14 days (b) NMDE is located in a valley in southwest New Mexico (see Figure 2). The periodic annual amplitude of vertical deformation for the GNSS time series is around ± 20 mm, while the equivalent computed amplitudes for the GRACE and UASWE time series are lower, at ± 5 mm and -10 to 0 mm, respectively. The annual responses computed from GRACE TWS and the UASWE snowpack are significantly lower at this location, owing to station's distance is from the nearest high mountain range. The annual periodic signals in the GNSS and GRACE data sets are almost completely antiphase, with GRACE leading GNSS by 214 days, suggesting that station NMDE is sensitive to the snowmelt runoff that flows within its vicinity during the spring and summer months.

4.2. GNSS and UASWE Regression

The result of the least-squares regression between the observed GNSS and computed UASWE vertical displacement time series is shown in Figure 5. The variance in GNSS vertical displacement data explained by vertical displacement computed from the UASWE data set for most stations is below 10%. For some sub-regions, especially in the Wasatch Range and the Rocky Mountains, 20%–30% of the variance observed at many stations is explained by the UASWE data set. These station locations primarily correlate with the mountainous regions of the study area. A handful of stations have around 50% of their variance explained by the UASWE data set. These stations are highly sensitive to the accumulation and melt of the local snowpack.

4.3. GRACE and UASWE Regression

As seen in Figure 6, the least-squares regression between the computed GRACE and UASWE vertical displacement time series is significantly more uniform than the regression shown in Figure 5. This is to be expected, as the GRACE TWS data set has low spatial resolution, and most of the pixels in the study area behave coherently. Most station locations have GRACE vertical displacement time series variance that are explained by variance in the UASWE vertical displacement time series in excess of 40%, and many of these stations have values around 50%. The only sub-regions where the GRACE TWS data shows significant divergence from the UASWE data are the areas in southern and northwestern Arizona. These locations are sufficiently far away enough from the mountainous parts of the study region and their associated watersheds that the stations' signals are not coupled to the region's snowpack. Given that the variance in GRACE vertical displacement data explained by the variance in UASWE vertical displacement data in these sub-regions Arizona is around 10%, these stations might be decoupled from the broader hydrological processes of the study region and may reflect some sensitivity to elastic deformation resulting from precipitation from the North American Monsoon.

5. Discussion

5.1. Hydrological Implications

As seen in Figure 4, GNSS stations in and around mountainous areas of the Southwest United States respond to elastic deformation due to surface water loading months in advance of GNSS stations in low-lying and desert areas. GNSS stations in Colorado and Utah sense the accumulation of snow in fall and winter months, while stations in Arizona sense the runoff from the melting snowpack in the lower parts of mountain watersheds during spring months. The negative phase delay anomaly in New Mexico likely does not represent a real physical feature, as it is heavily skewed by several negative-valued station locations contained within it. Ignoring this feature, a two-lobed pattern of phase delays emerges, with a negative lobe in the north and northeast parts of the study region, and a positive lobe in the southwest portion. It is important to note that, due to the low spatial resolution of GRACE TWS data, it provides only a snapshot into broad regional hydrological processes. By combining information about elastic deformation from both GRACE and GNSS, details about watershed-scale hydrological processes materialize.

The overall low variance explanation from the UASWE data set, as seen in Figure 5, is due to the fact that this data set records only the accumulation and removal of snow in the snowpack itself. It does not provide information about the redistribution of snowpack meltwater that forms in the spring months. Figure 5 demonstrates that a large

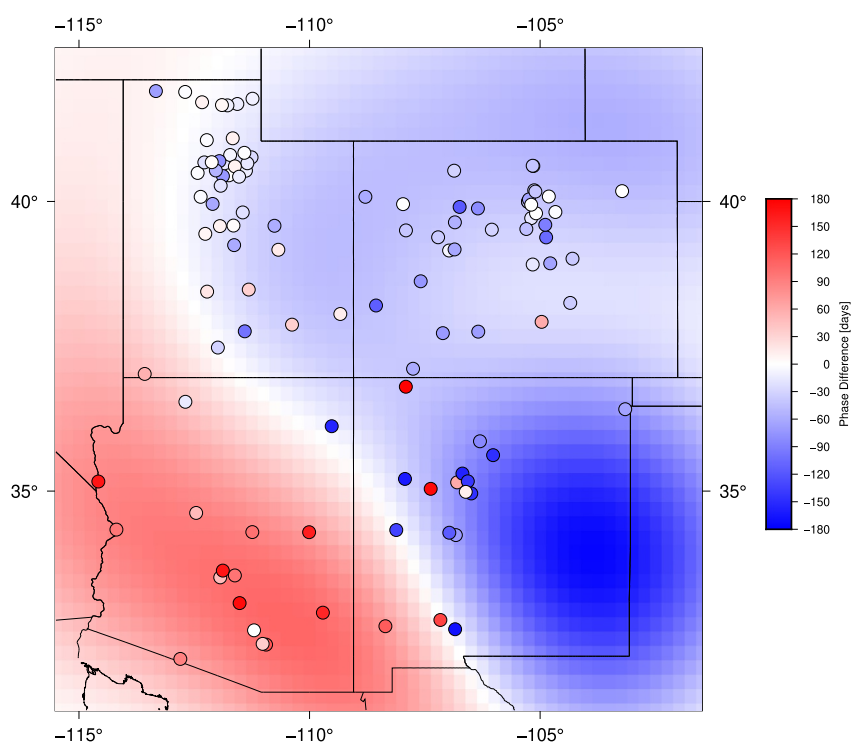


Figure 4. Map of temporal phase delays between the observed GNSS and computed GRACE vertical displacement data sets. The phase delay at individual station locations is plotted as filled circles. The long-wavelength response computed by projecting the location responses into the regional Slepian basis is plotted across the entire map. A negative phase delay (blue) indicates that the annual periodic signal of GNSS is leading that of GRACE, while a positive phase delay (red) indicates that the GRACE signal is leading that of GNSS. There exists a strong degree two signal in the regional phase delays: GNSS stations sense hydrological loading in the mountainous regions one to two months before it appears in the GRACE gravimetry data, while this relative timing flip-flops in the lower Colorado River Basin.

portion of the GNSS stations in the study area are more sensitive to the surface elastic deformation that results from the local accumulation of meltwater as opposed to changes in the snowpack itself. The GNSS stations essentially act as spatial high-pass filters for the elastic deformation, as they are responsive to TWS variations only within tens of kilometers, as suggested by these results. They can provide much higher resolution TWS data for a hydrologically complex region such as the Southwest United States, even though the station density is sparse and irregular.

Besides variations in TWS, the data in this study provides useful information about other climate trends and phenomena. As mentioned previously, one of the most pertinent contributions to TWS in the study area besides snow accumulation and melt is the North American Monsoon. One interesting result to emerge from the analyses in this study is the identification of a subset of GNSS stations whose vertical displacement is decoupled from changes in the snowpack relative to the majority of the stations in this study. These stations in southern and northwestern Arizona, as highlighted in Figure 6, should be investigated for their relationship to monsoonal precipitation.

Near-real-time monitoring of TWS is becoming increasingly important as the effects of anthropogenic climate change increase in severity (Jiang et al., 2021). This is especially apparent in the study area, where water storage along the Colorado River is reaching extreme lows (Adusumilli et al., 2019). Instead of relying on streamflow measurements during the spring months, models of elastic deformation that incorporate GNSS vertical displacement and Gravity Recovery and Climate Experiment Follow-On (GRACE-FO) TWS data can help refine estimates of the snowpack in the source regions of the Colorado River during the fall and winter months. This would help governments that rely on the Colorado River for water to plan water savings and other emergency measures months in advance of a water shortage.

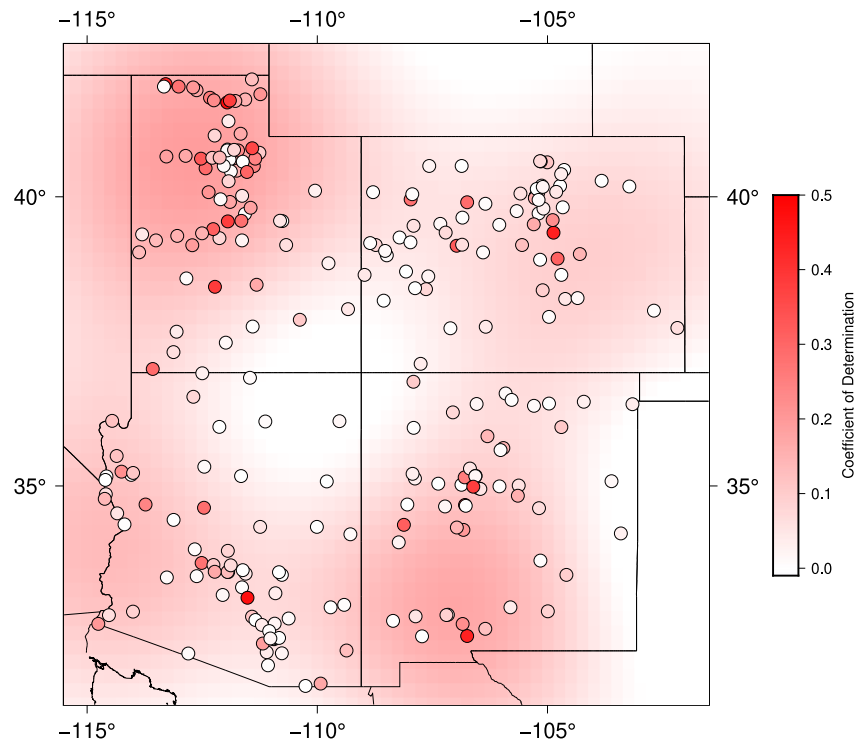


Figure 5. Map of the R^2 value (coefficient of determination) that results from performing a least-squares regression between the observed GNSS and computed UASWE vertical displacement time series values at each station location. The R^2 value at each individual station location is plotted as a filled circle, and the response computed by projecting the site responses into the regional Slepian basis is plotted across the entire map. There is little coherence between the two data sets across the study area, as only about 30 locations have an R^2 value above 0.2. The relative GNSS station spacing is reflected in the regional projection, as the background map has the highest values in the sub-regions with the densest populations of stations, while the center of the region has the fewest stations and therefore the lowest R^2 values.

A high density of GNSS stations is critical to monitoring changes in TWS throughout a region (Han & Razeqhi, 2017; Knappe et al., 2019). However, the results of this study suggest that it is possible to partially complement areas of sparse GNSS networks with snowpack SWE models in mountainous regions, such as the Western United States. These snowpack SWE models provide information about snow accumulation and melt, which is critical to understanding surface elastic deformation in the mountain ranges that receive snow. This same information is not fully conveyed by GNSS station vertical displacement data, as suggested by Figure 5. On the other hand, GNSS stations in drainage areas around these mountain ranges provide data on the timing and magnitude of snowmelt runoff. These stations sense the accumulation and melt of snow 1 to 3 months in advance of GRACE TWS in the Southwest United States, as suggested by our results here. The placement of GNSS stations in different segments of larger watersheds is integral to understanding TWS variations at the watershed basin scale.

5.2. Sources of Error

When comparing the magnitudes of error between the three data sets used in this study, GNSS station vertical displacement data dominates both GRACE TWS and UASWE. The maximum magnitude of GNSS data error can exceed 4 mm/yr at some stations, while the error of both GRACE TWS and UASWE stay below 1 mm/yr. It is important to take into account the various sources of GNSS station displacement data error, which include common mode (Bogusz et al., 2024); atmospheric delay modeling (Tregoning et al., 2009); site-specific thermal expansion (Fang et al., 2013; Yan et al., 2009); poroelastic strain due to groundwater (Tsai, 2011); and other non-tidal errors (Gu et al., 2017). Previous studies also removed stations from their analyses whose locations have large local soil expansion and contraction responses due to changes in groundwater storage (e.g., Argus et al., 2014, 2017). No such selectivity is performed in this study, as there is a lack of community agreement on

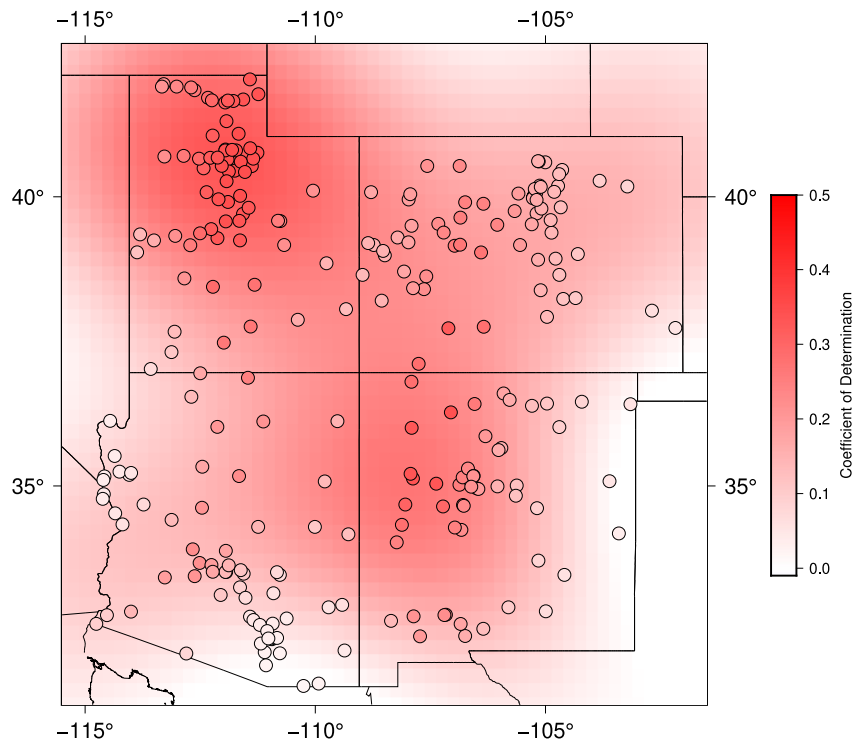


Figure 6. Same as Figure 5 but for the R^2 values that result from the linear regression between the computed GRACE and UASWE vertical displacement time series values at each station. In contrast to Figure 5, there is strong coherence between the two data sets across the study area at most sites. This suggests that the snowpack provides a first-order control on GRACE TWS data. The only exceptions are two groups of stations in southern Arizona and along the Colorado River in western Arizona. These groups of stations have R^2 values near 10%, suggesting that they are not highly controlled by variations in the snowpack.

how site-specific processes are coupled to GNSS displacement and how to filter for them. It is likely that the stations that display large discrepancies in their signal content compared to GRACE are biased by one or more of the site-specific errors listed above. Future analyses using this GNSS vertical displacement data set will first remove stations with high variability in their response to surface water loading using a methodology similar to Argus et al. (2017). GNSS station displacement errors other than the ones mentioned will also be considered, such as those summarized in Dong et al. (2002).

6. Conclusions and Future Directions

In this study, we perform the first region-specific analysis and comparison of GNSS vertical displacement, GRACE TWS, and snowpack SWE data sets for the southwest United States. We observe a location-dependent phase delay between GNSS and GRACE vertical displacement data, demonstrating that snow accumulation and melt in mountainous regions provide a first-order control on elastic deformation of Earth's surface in this study area. In the Wasatch Range, GNSS stations sense loading due to changes in the snowpack one to 2 months in advance of GRACE; in the Southern Rocky Mountains, GNSS stations sense loading due to changes in the snowpack one to 3 months in advance of GRACE; and in the lower Colorado River Basin, GRACE senses loading due to changes in river runoff three or more months in advance of GNSS stations. This comparison of these three geodetic data sets allows us to view the broad hydrological partitioning between mountains and rivers in these three sub-regions of the Colorado River Basin. Hydrological surface loading from the North American Monsoon is also suggested as a second-order control on the observed displacement at GNSS stations in southern and northwestern Arizona. Variations in the UASWE snowpack SWE coverage data set are observed to have little control over variations in GNSS vertical displacement data, indicating that GNSS stations in the study region have a hyper-local sensitivity to variations in the distribution of TWS surface mass. A model of the redistribution of snowmelt runoff in individual watersheds is needed to complement TWS deficiencies in the UASWE data set.

The ultimate goal of this line of work is to create a model of sub-monthly variations in TWS with a spatial resolution of tens of kilometers in the study region. This will involve a joint inversion of GNSS and GRACE data sets, similar to Han and Razeghi (2017) and Knappe et al. (2019). A snowpack SWE data set will also be necessary for the analysis, as demonstrated by this study, to provide the desired spatial resolution. That being said, the snowpack SWE data set does not make up for the station sparsity in low elevation areas of the study region. In order to model the redistribution of snowmelt runoff throughout the study region, another TWS data set is required. One such candidate data set is the Global Land Data Assimilation System (GLDAS), which provides 1 km resolution land-based grids of changes in surface water resources (Rodell et al., 2004). This data set could be incorporated in a joint analysis, although previous studies (e.g., Fu et al., 2015; Knappe et al., 2019) suggest that GLDAS has a limited representation of the water cycle and provides little information that is independent of SWE data sets. Future analyses will involve attempting to separate the seasonal signal of the North American Monsoon from the annual signal of snow accumulation and melt in the Southwest United States. A focus on other climate patterns, such as the El Niño-Southern Oscillation and atmospheric rivers, may also prove fruitful (Adusumilli et al., 2019).

Conflict of Interest

The authors declare no conflicts of interest relevant to this study.

Data Availability Statement

The code used in this work is available freely online (Harig et al., 2015) as part of the SLEPIAN code package. Specifically Slepian_alpha (Simons et al., 2020) and Slepian_bravo (Simons & Harig, 2020) are used to generate and work with Slepian functions, while Slepian_delta (Harig & Simons, 2022) processes GRACE data. Installation instructions for the various Slepian code repositories can be found at <http://github.com/Slepian/Slepian> (Plattner et al., 2023). The GNSS time series (Blewitt et al., 2018) used for processing in this study are available from the University of Nevada Reno Nevada Geodetic Laboratory (<http://geodesy.unr.edu/>) under open access. Individual GNSS station time series data sets and access are outlined at <http://geodesy.unr.edu/PlugNPlayPortal.php>. Version 1.9 of Hector (Bos et al., 2013) used to compute linear displacement trends for the GNSS time series is available via the GNU General License at <https://segal.ubi.pt/webservices/whatishector/>. The CSR RL06 GRACE time series used for processing in this study are freely available at The NASA Physical Oceanography Distributed Active Archive Center (PO.DAAC) (<https://podaac.jpl.nasa.gov/>). The data can be accessed via NASA EarthData Search at <https://dx.doi.org/10.5067/GRGSM-20C06>. The gridded SWE data set (Broxton et al., 2019) is freely available at the National Snow and Ice Data Center and can be accessed at <https://doi.org/10.5067/0GGPB220EX6A>. LoadDef (Martens et al., 2019), used to compute surface elastic displacement due to changes in water loading, is available under the GNU General Public License v3.0 at <https://github.com/hrmartens/LoadDef>.

Acknowledgments

The authors would like to thank Dr. Jeffrey T. Freymueller; two anonymous reviewers; and the editor, Dr. Di Long for their constructive comments and suggestions. CH acknowledges support from the National Science Foundation (NSF) via Grant NSF-2142980 funded by the Geophysics program. Figures were plotted using the Generic Mapping Tools (Wessel et al., 2013).

References

- Adusumilli, S., Borsa, A. A., Fish, M. A., McMillan, H. K., & Silverii, F. (2019). A decade of water storage changes across the contiguous United States from GPS and satellite gravity. *Geophysical Research Letters*, *46*(22), 13006–13015. <https://doi.org/10.1029/2019GL085370>
- Altamimi, Z., Rebischung, P., Métivier, L., & Collilieux, X. (2016). ITRF2014: A new release of the international terrestrial reference frame modeling nonlinear station motions. *Journal of Geophysical Research: Solid Earth*, *121*(8), 6109–6131. <https://doi.org/10.1002/2016JB013098>
- Argus, D. F., Fu, Y., & Landerer, F. W. (2014). Seasonal variation in total water storage in California inferred from GPS observations of vertical land motion. *Geophysical Research Letters*, *41*(6), 1971–1980. <https://doi.org/10.1002/2014GL059570>
- Argus, D. F., Landerer, F. W., Wiese, D. N., Martens, H. R., Fu, Y., Famiglietti, J. S., et al. (2017). Sustained water loss in California's Mountain ranges during severe drought from 2012 to 2015 inferred from GPS. *Journal of Geophysical Research: Solid Earth*, *122*(12), 10559–10585. <https://doi.org/10.1002/2017JB014424>
- Beveridge, A. K., Harig, C., & Simons, F. J. (2018). The changing mass of glaciers on the Tibetan Plateau, 2002–2016, using time-variable gravity from the GRACE satellite mission. *Journal of Geodetic Science*, *8*, 1–15. <https://doi.org/10.1515/jogs-2018-0010>
- Blewitt, G., Hammond, W., & Kreemer, C. (2018). Harnessing the GPS data explosion for interdisciplinary science [Dataset]. *Eos*, *99*. <https://doi.org/10.1029/2018eo104623>
- Blewitt, G., Lavallée, D., Clarke, P., & Nurutdinov, K. (2001). A new global mode of Earth deformation: Seasonal cycle detected. *Science*, *294*(5550), 2342–2345. <https://doi.org/10.1126/science.1065328>
- Bogusz, J., Rebischung, P., & Klos, A. (2024). Differences in annual signals between IGS- and NGL-derived position time series: Testing different strategies of alignment to the reference frame. In *EGU general assembly 2024*. <https://doi.org/10.5194/egusphere-egu24-5351>
- Bos, M. S., Fernandes, R. M., Williams, S. D., & Bastos, L. (2013). Fast error analysis of continuous GNSS observations with missing data [Software]. *Journal of Geodesy*, *87*(4), 351–360. <https://doi.org/10.1007/s00190-012-0605-0>

- Broxton, P. D., Dawson, N., & Zeng, X. (2016). Linking snowfall and snow accumulation to generate spatial maps of SWE and snow depth. *Earth and Space Science*, 3(6), 246–256. <https://doi.org/10.1002/2016EA000174>
- Broxton, P. D., Zeng, X., & Dawson, N. (2019). Daily 4 km gridded SWE and snow depth from assimilated in-situ and modeled data over the conterminous us (NSIDC-0719, version 1) [Dataset]. *NASA National Snow and Ice Data Center Distributed Active Archive Center*. <https://doi.org/10.5067/0GGPB220EX6A>
- Carlson, G., Werth, S., & Shirzaei, M. (2022). Joint inversion of GNSS and GRACE for terrestrial water storage change in California. *Journal of Geophysical Research: Solid Earth*, 127(3), e2021JB023135. <https://doi.org/10.1029/2021jb023135>
- Chanard, K., Métois, M., Rebeschung, P., & Avouac, J.-P. (2020). A warning against over-interpretation of seasonal signals measured by the global navigation satellite system. *Nature Communications*, 11(1), 1375. <https://doi.org/10.1038/s41467-020-15100-7>
- Davis, J. L., Elósegui, P., Mitrovica, J. X., & Tamisiea, M. E. (2004). Climate-driven deformation of the solid Earth from GRACE and GPS. *Geophysical Research Letters*, 31(24), 1–4. <https://doi.org/10.1029/2004GL021435>
- Dong, D., Fang, P., Bock, Y., Cheng, M. K., & Miyazaki, S. (2002). Anatomy of apparent seasonal variations from GPS-derived site position time series. *Journal of Geophysical Research*, 107(B4), 1–16. <https://doi.org/10.1029/2001jb000573>
- Dziewonski, A. M., & Anderson, D. L. (1981). Preliminary reference Earth model. *Physics of the Earth and Planetary Interiors*, 25(4), 297–356. [https://doi.org/10.1016/0031-9201\(81\)90046-7](https://doi.org/10.1016/0031-9201(81)90046-7)
- Enzinger, T. L., Small, E. E., & Borsa, A. A. (2018). Accuracy of snow water equivalent estimated from GPS vertical displacements: A synthetic loading case study for Western U.S. Mountains. *Water Resources Research*, 54(1), 581–599. <https://doi.org/10.1002/2017WR021521>
- Enzinger, T. L., Small, E. E., & Borsa, A. A. (2019). Subsurface water dominates Sierra Nevada seasonal hydrologic storage. *Geophysical Research Letters*, 46(21), 11993–12001. <https://doi.org/10.1029/2019GL084589>
- Fang, M., Dong, D., & Hager, B. H. (2013). Displacements due to surface temperature variation on a uniform elastic sphere with its centre of mass stationary. *Geophysical Journal International*, 196(1), 194–203. <https://doi.org/10.1093/gji/ggt335>
- Farrell, W. E. (1972). Deformation of the Earth by surface loads. *Reviews of Geophysics*, 10(3), 761–797. <https://doi.org/10.1029/RG010i003p00761>
- Fu, Y., Argus, D. F., & Landerer, F. W. (2015). GPS as an independent measurement to estimate terrestrial water storage variations in Washington and Oregon. *Journal of Geophysical Research: Solid Earth*, 120, 552–566. <https://doi.org/10.1002/2014JB011415>. Received
- Gu, Y., Fan, D., & You, W. (2017). Comparison of observed and modeled seasonal crustal vertical displacements derived from multi-institution GPS and GRACE solutions. *Geophysical Research Letters*, 44(14), 7219–7227. <https://doi.org/10.1002/2017GL074264>
- Han, S. C., & Razeghi, S. M. (2017). GPS recovery of daily hydrologic and atmospheric mass variation: A methodology and results from the Australian continent. *Journal of Geophysical Research: Solid Earth*, 122(11), 9328–9343. <https://doi.org/10.1002/2017JB014603>
- Harig, C., Lewis, K. W., Plattner, A., & Simons, F. J. (2015). A suite of software analyzes data on the sphere [Software]. *Eos*, 96. <https://doi.org/10.1029/2015EO025851>
- Harig, C., & Simons, F. J. (2012). Mapping Greenland's mass loss in space and time. *Proceedings of the National Academy of Sciences of the United States of America*, 109(49), 19934–19937. <https://doi.org/10.1073/pnas.1206785109>
- Harig, C., & Simons, F. J. (2015). Accelerated West Antarctic ice mass loss continues to outpace East Antarctic gains. *Earth and Planetary Science Letters*, 415, 134–141. <https://doi.org/10.1016/j.epsl.2015.01.029>
- Harig, C., & Simons, F. J. (2016). Ice mass loss in Greenland, the Gulf of Alaska, and the Canadian Archipelago: Seasonal cycles and decadal trends. *Geophysical Research Letters*, 43(7), 3150–3159. <https://doi.org/10.1002/2016GL067759>
- Harig, C., & Simons, F. J. (2022). csdms-contrib/slepian_delta: Release 1.2.1 [Software]. *Zenodo*. <https://doi.org/10.5281/zenodo.6562354>
- Jaramillo, F., Aminjafari, S., Castellazzi, P., Fleischmann, A., Fluet-Chouinard, E., Hashemi, H., et al. (2024). The potential of hydrogeodesy to address water-related and sustainability challenges. *Water Resources Research*, 60(11), e2023WR037020. <https://doi.org/10.1029/2023WR037020>
- Jiang, Z., Hsu, Y. J., Yuan, L., Yang, X., Ding, Y., Tang, M., & Chen, C. (2021). Characterizing spatiotemporal patterns of terrestrial water storage variations using GNSS vertical data in Sichuan, China. *Journal of Geophysical Research: Solid Earth*, 126(12), e2021JB022398. <https://doi.org/10.1029/2021JB022398>
- Knappe, E., Bendick, R., Martens, H. R., Argus, D. F., & Gardner, W. P. (2019). Downscaling vertical GPS observations to derive watershed-scale hydrologic loading in the Northern Rockies. *Water Resources Research*, 55(1), 391–401. <https://doi.org/10.1029/2018WR023289>
- Knowles, L., Bennett, R. A., & Harig, C. (2020). Vertical displacements of the Amazon basin from GRACE and GPS. *Journal of Geophysical Research: Solid Earth*, 125(2), e2019JB018105. <https://doi.org/10.1029/2019JB018105>
- Landerer, F. W., & Swenson, S. C. (2012). Accuracy of scaled GRACE terrestrial water storage estimates. *Water Resources Research*, 48(4), 1–11. <https://doi.org/10.1029/2011WR011453>
- Loomis, B. D., Rachlin, K. E., Wiese, D. N., Landerer, F. W., & Luthecke, S. B. (2020). Replacing GRACE/GRACE-FO with satellite laser ranging: Impacts on Antarctic ice sheet mass change. *Geophysical Research Letters*, 47(3), e2019GL085488. <https://doi.org/10.1029/2019GL085488>
- Love, A. E. H. (1909). The yielding of the Earth to disturbing forces. *Proceedings of the Royal Society of London. Series A*, 82(551), 73–88. <https://doi.org/10.1098/rspa.1909.0008>
- Martens, H. R., Rivera, L., & Simons, M. (2019). LoadDef: A python-based toolkit to model elastic deformation caused by surface mass loading on spherically symmetric bodies [Software]. *Earth and Space Science*, 6(2), 311–323. <https://doi.org/10.1029/2018EA000462>
- Ouellette, K. J., De Linage, C., & Famiglietti, J. S. (2013). Estimating snow water equivalent from GPS vertical site-position observations in the western United States. *Water Resources Research*, 49(5), 2508–2518. <https://doi.org/10.1002/wrcr.20173>
- Pedregosa, F., Varoquaux, G., Michel, V., Thirion, B., Grisel, O., Blondel, M., et al. (2011). Scikit-learn: Machine learning in python. *Journal of Machine Learning Research*, 12, 2825–2830. <https://doi.org/10.1289/EHP4713>
- Plattner, A., Kroeker, S., & Kylejeford, H., & RamonRich. (2023). Slepian/slepian: V1.2.0 [Software]. *Zenodo*. <https://doi.org/10.5281/zenodo.7838064>
- Ray, J., Altamimi, Z., Collilieux, X., & van Dam, T. (2007). Anomalous harmonics in the spectra of GPS position estimates. *GPS Solutions*, 12(1), 55–64. <https://doi.org/10.1007/s10291-007-0067-7>
- Rebeschung, P., Altamimi, Z., Métivier, L., Gobron, K., & Chanard, K. (2024). Analysis of the IGS contribution to ITRF2020. *Journal of Geodesy*, 98(49). <https://doi.org/10.1007/s00190-024-01870-1>
- Rodell, M., Houser, P. R., Jambor, U., Gottschalck, J., Mitchell, K., Meng, C. J., et al. (2004). The global land data assimilation system. *Bulletin American Meteorology Soc*, 85(3), 381–394. <https://doi.org/10.1175/BAMS-85-3-381>
- Serreze, M. C., Clark, M. P., Armstrong, R. L., McGinnis, D. A., & Pulwarty, R. S. (1999). Characteristics of the western United States snowpack from snowpack telemetry (SNOTEL) data. *Water Resources Research*, 35(7), 2145–2160. <https://doi.org/10.1029/1999WR900090>

- Simons, F. J., & Dahlen, F. A. (2006). Spherical Slepian functions and the polar gap in geodesy. *Geophysical Journal International*, 166(3), 1039–1061. <https://doi.org/10.1111/j.1365-246X.2006.03065.x>
- Simons, F. J., & Harig, C. (2020). csdms-contrib/slepian_bravo: Release 1.0.4 [Software]. *Zenodo*. <https://doi.org/10.5281/zenodo.4085221>
- Simons, F. J., Harig, C., & Plattner, A. (2020). csdms-contrib/slepian_alpha: Release 1.0.5 [Software]. *Zenodo*. <https://doi.org/10.5281/zenodo.4085210>
- Sun, Y., Riva, R., & Ditmar, P. (2016). Optimizing estimates of annual variations and trends in geocenter motion and j_2 from a combination of grace data and geophysical models. *Journal of Geophysical Research: Solid Earth*, 121(11), 8352–8370. <https://doi.org/10.1002/2016JB013073>
- Swenson, S. C., Chambers, D., & Wahr, J. (2008). Estimating geocenter variations from a combination of grace and ocean model output. *Journal of Geophysical Research*, 113(B8). <https://doi.org/10.1029/2007JB005338>
- Swenson, S. C., & Wahr, J. (2006). Post-processing removal of correlated errors in GRACE data. *Geophysical Research Letters*, 33(8), 1–4. <https://doi.org/10.1029/2005GL025285>
- Tapley, B. D., Bettadpur, S., Ries, J. C., Thompson, P. F., & Watkins, M. M. (2004). GRACE measurements of mass variability in the Earth system. *Science*, 305(5683), 503–505. <https://doi.org/10.1126/science.1099192>
- Tregoning, P., & Watson, C. (2009). Atmospheric effects and spurious signals in GPS analyses. *Journal of Geophysical Research*, 114(9), 1–15. <https://doi.org/10.1029/2009JB006344>
- Tregoning, P., Watson, C., Ramillien, G., McQueen, H., & Zhang, J. (2009). Detecting hydrologic deformation using GRACE and GPS. *Geophysical Research Letters*, 36(15), 1–6. <https://doi.org/10.1029/2009GL038718>
- Tsai, V. C. (2011). A model for seasonal changes in GPS positions and seismic wave speeds due to thermoelastic and hydrologic variations. *Journal of Geophysical Research*, 116(4), 1–9. <https://doi.org/10.1029/2010JB008156>
- van Dam, T., Wahr, J., & Lavallée, D. (2007). A comparison of annual vertical crustal displacements from GPS and gravity recovery and climate experiment (GRACE) over Europe. *Journal of Geophysical Research*, 112(3), 1–11. <https://doi.org/10.1029/2006JB004335>
- von Hippel, M., & Harig, C. (2019). Long-term and inter-annual mass changes in the Iceland ice cap determined from GRACE gravimetry using Slepian functions. *Frontiers in Earth Science*, 7(171), 1–10. <https://doi.org/10.3389/feart.2019.00171>
- Wahr, J., Molenaar, M., & Bryan, F. (1998). Time variability of the Earth's gravity field: Hydrological and oceanic effects and their possible detection using GRACE. *Journal of Geophysical Research*, 103(B12), 30205–30229. <https://doi.org/10.1029/98jb02844>
- Wessel, P., Smith, W. H. F., Scharroo, R., Luis, J., & Wobbe, F. (2013). Generic mapping tools: Improved version released. *Eos, Transactions American Geophysical Union*, 94(45), 409–410. <https://doi.org/10.1002/2013EO450001>
- White, A. M., Gardner, W. P., Borsa, A. A., Argus, D. F., & Martens, H. R. (2022). A review of GNSS/GPS in hydrogeodesy: Hydrologic loading applications and their implications for water resource research. *Water Resources Research*, 58(7), e2022WR032078. <https://doi.org/10.1029/2022WR032078>
- Yan, H., Chen, W., Zhu, Y., Zhang, W., & Zhong, M. (2009). Contributions of thermal expansion of monuments and nearby bedrock to observed GPS height changes. *Geophysical Research Letters*, 36(13), 1–5. <https://doi.org/10.1029/2009GL038152>
- Zeng, X., Broxton, P. D., & Dawson, N. (2018). Snowpack change from 1982 to 2016 over conterminous United States. *Geophysical Research Letters*, 45(23), 12940–12947. <https://doi.org/10.1029/2018GL079621>